Molecular Plant
Research Article

CellPress
PARTNER JOURNAL

An INDEHISCENT-Controlled Auxin Response Specifies the Separation Layer in Early *Arabidopsis* Fruit

Kasper van Gelderen[1,2,3], Martin van Rongen[1,2,4], An'an Liu[1], Anne Otten[1] and Remko Offringa[1,*]

[1]Molecular and Developmental Genetics, Institute of Biology Leiden, Leiden University, Sylviusweg 72, 2333 BE Leiden, the Netherlands

[2]These authors contributed equally to this article.

[3]Present address: Plant Ecophysiology, Institute of Environmental Biology, Utrecht University, 3584 CH Utrecht, the Netherlands

[4]Present address: Sainsbury Laboratory, 47 Bateman Street, Cambridge CB2 1LR, UK

***Correspondence: Remko Offringa (r.offringa@biology.leidenuniv.nl)**

http://dx.doi.org/10.1016/j.molp.2016.03.005

ABSTRACT

Seed dispersal is an important moment in the life cycle of a plant species. In *Arabidopsis thaliana*, it is dependent on transcription factor INDEHISCENT (IND)-mediated specification of a separation layer in the dehiscence zone found in the margin between the valves (carpel walls) and the central replum of the developing fruit. It was proposed that IND specifies the separation layer by inducing a local auxin minimum at late stages of fruit development. Here we show that morphological differences between the *ind* mutant and wild-type fruit already arise at early stages of fruit development, coinciding with strong *IND* expression in the valve margin. We show that IND-reduced PIN-FORMED3 (PIN3) auxin efflux carrier abundance leads to an increased auxin response in the valve margin during early fruit development, and that the concomitant cell divisions that form the dehiscence zone are lacking in *ind* mutant fruit. Moreover, *IND* promoter-driven ectopic expression of the AGC kinases PINOID (PID) and WAG2 induced indehiscence by expelling auxin from the valve margin at stages 14–16 of fruit development through increased PIN3 abundance. Our results show that IND, besides its role at late stages of *Arabidopsis* fruit development, functions at early stages to facilitate the auxin-triggered cell divisions that form the dehiscence zone.

Key words: seed dispersal, polar auxin transport, PINOID, INDEHISCENT, separation layer, *Arabidopsis*

van Gelderen K., van Rongen M., Liu A., Otten A., and Offringa R. (2016). An INDEHISCENT-Controlled Auxin Response Specifies the Separation Layer in Early *Arabidopsis* Fruit. Mol. Plant. **9**, 857–869.

INTRODUCTION

Correct timing of fruit and seed ripening and the subsequent dispersal of the seeds is important to ensure the survival of the next plant generation. This also requires proper patterning of the gynoecium from which the fruit develops. The *Arabidopsis* gynoecium, and that of other Brassicaceae, consists of two fused carpels that form the valves. The valves are fused by a valve margin and replum, which is connected internally to the septum and ovules. The valve margins delimit the borders between valves and replum and consist of a separation layer and a layer of lignified cells (Ferrándiz, 2002). At the final stage of fruit development, cells within the separation layer secrete cell-wall-degrading enzymes that promote cell separation, and the rigidity of the lignified layer aids the separation of the valves from the replum. This process is referred to as dehiscence and results in seed dispersal (for a review, see Østergaard, 2009). The valve margin is specified by expression of the valve margin identity genes *INDEHISCENT* (*IND*), *SHATTERPROOF* (*SHP1/2*), and *ALCATRAZ* (*ALC*), which is limited to a narrow region on the valve/replum border due to the repressing effect of FRUITFULL (FUL) in the valves and REPLUMLESS (RPL) in the replum (Ferrándiz et al., 2000; Roeder et al., 2003). Subsequent differentiation of the dehiscence zone into a separation layer and a lignified layer is determined by SHP1/2 and IND, whereas separation layer specification also requires ALC (Ferrándiz et al., 2000; Rajani and Sundaresan, 2001; Liljegren et al., 2004; Girin et al., 2011).

Published by the Molecular Plant Shanghai Editorial Office in association with Cell Press, an imprint of Elsevier Inc., on behalf of CSPB and IPPE, SIBS, CAS.

Previously, it has been reported that the basic helix-loop-helix (bHLH) transcription factor IND is responsible for the formation of an auxin minimum in the dehiscence zone of the fruit at stage 17B and that this auxin minimum is required for separation layer specification (Sorefan et al., 2009). Members of the PIN-FORMED (PIN) family of auxin efflux carriers have been proposed to play an important role in the establishment of this auxin minimum, as overexpression of IND in seedlings was found to lead to PIN1 and PIN3 polarity loss. IND and the bHLH transcription factor SPATULA (SPT) were found to bind the promoters of the AGC kinase genes *PINOID* (*PID*) and *WAG2* and to repress the expression of *PID* and upregulate the expression of *WAG2* in seedlings and developing fruits (Sorefan et al., 2009; Girin et al., 2011). Since the PID and WAG2 protein kinases are well-established determinants in the subcellular distribution of PIN proteins (Benjamins et al., 2001; Friml et al., 2004; Michniewicz et al., 2007; Dhonukshe et al., 2010), a model was proposed in which IND/SPT-mediated downregulation of PID prevents shootward relocalization of PIN3, whereas enhanced *WAG2* expression promotes lateralization of PIN3, which is necessary to obtain the auxin minimum in the dehiscence zone. This model suggested that PID and WAG2 kinases act antagonistically on PIN3 polarity (Sorefan et al., 2009). However, in other publications, PID, WAG1, and WAG2 were shown to act redundantly to promote apical PIN1 localization in the embryo protoderm, shootward PIN2 localization in the root tip (Dhonukshe et al., 2010), or PIN3 outer lateral abundance in hypocotyl endodermis cells (Ding et al., 2011).

In order to further investigate the possible antagonistic role of the PID and WAG2 kinases in dehiscence zone specification, we assessed valve margin specification and fruit opening in plants with altered kinase activity. First, since there is contrasting data on when dehiscence zone differentiation is initiated (Wu et al., 2006; Sorefan et al., 2009), and since a detailed overview of its development is lacking, we traced valve margin and dehiscence zone development in wild-type fruit from before pollination up until fruit maturation. We compared this development with the *ind-2* mutant, which does not form a valve margin (Liljegren et al., 2004). We then closely investigated the role of auxin and its transport in the process of dehiscence zone differentiation, by visualizing auxin distribution and PIN3 localization at the valve margin in both wild-type and *ind-2* mutant background. Our results indicate that dehiscence zone formation takes place at stages 14–16 of fruit development and that this coincides with a reduction in PIN3 abundance and an increase in auxin levels in valve margin cells. Valve margin-specific expression of *PID* and *WAG2* resulted in indehiscence, which indicates that the reduced PIN3 plasma membrane abundance requires the expression of these redundantly acting AGC kinases to be repressed during dehiscence zone formation.

RESULTS

Dehiscence Zone Formation Is Initiated Following Pollination

The stages of gynoecium and fruit development important for dehiscence zone development are depicted in Figure 1A and 1B. *IND* is expressed throughout gynoecium and fruit development, including during the formation of an auxin minimum that develops immediately prior to fruit opening at stage 17B (Wu et al., 2006; Sorefan et al., 2009; Girin et al., 2011). Based on previous analyses, the formation of the dehiscence zone was suggested to occur through cell division events at stage 15 (Wu et al., 2006) (stages defined in Smyth et al., 1990). Since a detailed anatomical analysis of dehiscence zone formation has not been reported, we followed wild-type and *ind-2* fruit development from stages 11–17B through transverse sections of the center of the fruit. Up until the point of pollination at stage 13, an outline of the valve–replum border is becoming evident, possibly due to growth of neighboring tissue. However, our results did not reveal any obvious cell differentiation occurring in the valve margin up until the point of pollination at stage 13 (Figure 1C, Supplemental Figures 1A–1C and 2A–2C). Just after pollination, at stage 14, cell expansion of the epidermal valve cells and endocarp occurred and sutures started to form between the replum and valves (Figure 1D and 1L). Cell divisions that formed the smaller cells of the dehiscence zone started at stage 14 and continued into stages 15 and 16 (Figure 1F, 1G, and 1N). These cells continued to differentiate, forming the dehiscence zone at stage 17A and B (Figure 1I, 1J, and 1P). At these stages, the dehiscence zone could be identified based on the topology of the small separation layer cells and the more strongly stained lignified layer valve cells (Figure 1B, 1I, and 1J) (Ferrándiz et al., 1999). An earlier report suggested that the cell layers that are formed from stages 14–16 are the result of unequal (asymmetric) cell divisions (Wu et al., 2006), which would be in line with the notion that asymmetric cell divisions are formative and generate patterns (De Smet and Beeckman, 2011; Yoshida et al., 2014). Transverse sections indeed suggested that cell divisions in the valve margin might be unequal (Supplemental Figure 1D–1F). However, this may be an artifact of the shape of these cells, since they taper at the end (Supplemental Figure 1J), and therefore we were unable to unequivocally confirm the asymmetry of these divisions. Nonetheless, our results clearly indicated that dehiscence zone cell differentiation occurs early during fruit development, after fertilization at stages 14–16. In line with this observation, no discernible differences in cell topology at the valve margin between wild-type and *ind-2* fruits could be observed prior to fertilization (Figure 1C and 1E, Supplemental Figures 1A–1C and 2A–2C). However, the cell division and differentiation events occurring in this region after fertilization at stages 14–16 in wild-type fruit were completely absent in the *ind-2* mutant (Figure 1H and 1K, Supplemental Figures 1D–1F and 2D–2F). Our observations are in line with previous analyses (Wu et al., 2006), and show that dehiscence zone formation occurs as early as stage 14 of fruit development, directly after pollination (stage 13) by cell divisions between the valves and replum, producing one or two cell layers that continue to differentiate into the separation layer.

Auxin Levels Correlate with PIN3 Expression during Dehiscence Zone Formation

Our and previous data suggest that the dehiscence zone forms at stages 14–16 and therefore before the establishment of an auxin minimum at stage 17B. To investigate further the role of auxin during dehiscence zone formation, we traced auxin distribution from stages 11–17B in both wild-type and *ind-2* fruits, by correlating the auxin response reporters *DR5::RFP* (Benková et al.,

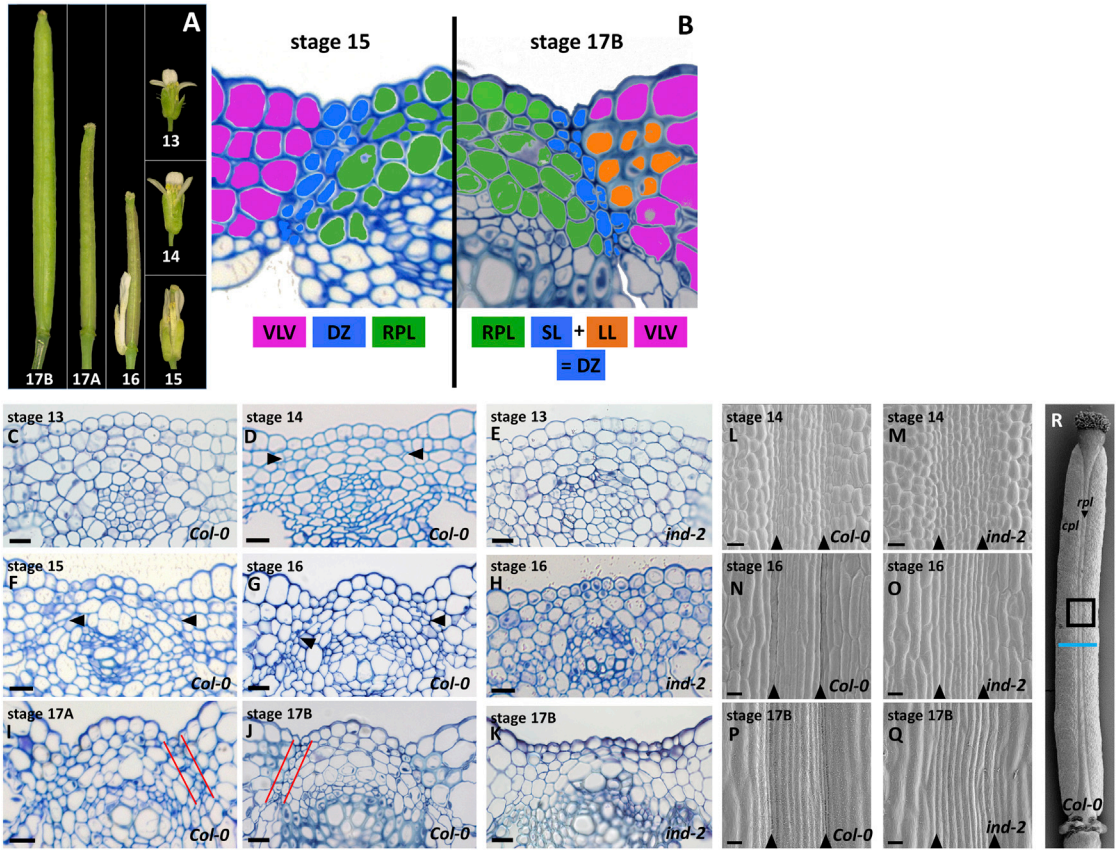

Figure 1. The Formation of the Dehiscence Zone Begins at Stage 14 of Fruit Development.

(A) *Arabidopsis* flowers at stage 13–17B of fruit development (Ferrándiz et al., 1999). At stage 13, the anthers extend to the stigmatic tissue and pollination takes place, while fertilization occurs at stage 14. The gynoecium starts to elongate and loses its floral parts from stage 15–17B after which the fruit ripens.

(B) Colored transverse sections of stage 15 and 17B fruit showing the valve (VLV, pink), replum (RPL, green) and the dehiscence zone (DZ, blue). At stage 17B, the DZ consists of the separation layer (SL, blue) and the lignified layer (LL, orange).

(C–K) Transverse sections of toluidine blue-stained *A. thaliana* fruit showing the replum and the valve margins. The blue bar in **(R)** indicates the approximate location of the sections in the fruit. Scale bar represents 10 μM.

(C and E) Stage 13 Col-0 **(C)** versus *ind-2* **(E)** gynoecium.

(D and F–H) In stage 14–16 Col-0 fruit **(D, F, and G)**, divisions (black arrowheads) create the smaller cells that form the dehiscence zone. These divisions or smaller cells are not visible in stage *ind-2* fruit **(H)**.

(I–K) In stage 17A and 17B fruit, the dehiscence zone (area between red lines) is clearly visible and the toluidine blue staining reveals the slight lignification of the lignified layer.

(L–R) Scanning electron microscopy images of stage 14, 16, and 17B Col-0 **(L, N, P, and R)** or *ind-2* **(M, O, and Q)** fruit. The position of the region shown in **(L–Q)** is indicated by the black box on the stage 17B fruit in **(R)**. The position of the valve margins, characterized by sutures in Col-0, are indicated by black arrowheads. Scale bar represents 10 μM.

2003) and *35S::DII-YFP* (Brunoud et al., 2012) with the plasma membrane localization of the predominant PIN in this region, PIN3 (Sorefan et al., 2009). *35S::DII-YFP* is an auxin sensor that operates through the auxin-mediated degradation of YFP fused to the IAA28 domain II (DII) degron. In the presence of auxin, the YFP signal decreases, which is opposite to the *DR5::RFP* reporter, where auxin enhances the RFP signal by activating the AUXIN RESPONSE FACTORS that are bound to the auxin response elements in the *DR5* promoter. The *35S::DII-YFP* reporter showed that at stage 13, during pollination, auxin was low in the valve, valve margin, and replum (Figure 2A). From stage 14–17A the DII-YFP signal gradually decreased in the valve margin, coinciding with a strong decrease in the replum and carpels (Figure 2B–2E). At stage 17B, the DII-YFP signal increased again, marking the previously reported auxin minimum in the valve margin (Sorefan et al., 2009) (Figure 2F). Parallel observations on the auxin-insensitive *35S::mDII-YFP* reporter showed that the *35S* promoter activity remained constant from stages 13–17A (Figure 2G–2H, 2N), corroborating that the observed decrease in DII-YFP signal during these stages is caused by an enhanced auxin response (Figure 2M and 2N). At stage 17B, the mDII-YFP signal strongly decreased, probably due the tissue growth occurring between stages 17A and 17B (the (m)DII-YFP signal was quantified over a range of cells and not by measuring single nuclei, see Methods). The DII-YFP/mDII-YFP signal ratio at stage 17B was similar to that at stage 13, indicating that an auxin response minimum was observed at both stages.

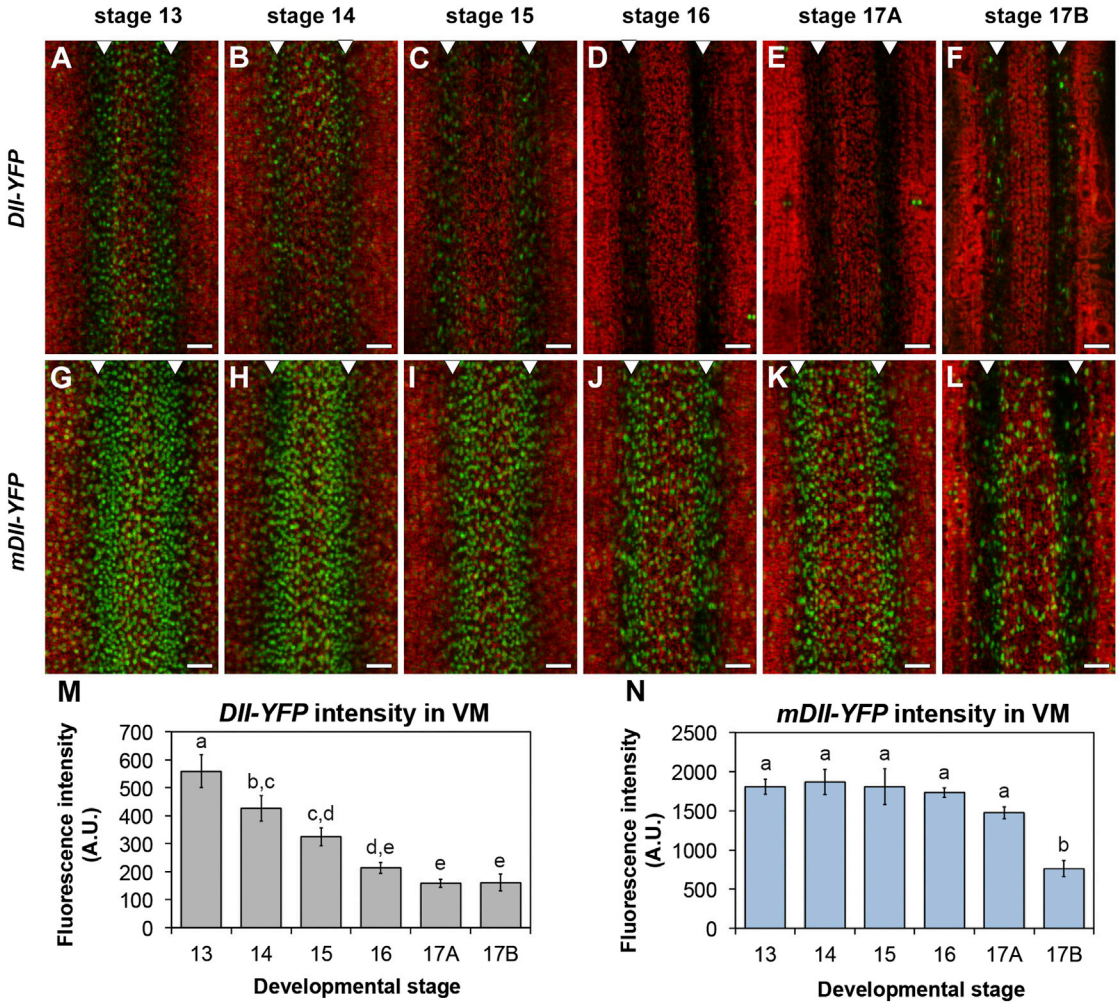

Figure 2. *DII-YFP*-Reported Auxin Increase in the Valve Margin at Early Stages of Fruit Development.
(A–N) SUM projection Z stack confocal microscopy images during development of the valve margin (white arrowheads) region of Col-0 *35S::DII:YFP-NLS* (*DII-YFP*) fruits **(A–F)** or Col-0 *35S::mDII:YFP-NLS* (m*DII-YFP*) fruits **(G–L)**. DII-YFP and mDII-YFP (green) levels in the valve margin (indicated by a white arrowhead) were quantified (**M and N**, respectively). For each stage, bars marked with different letters are significantly different from each other (ANOVA, $p < 0.05$). Fluorescence intensity levels are the mean total levels of eight individual valve margins. Error bars indicate the SE of the mean. The red signal is autofluorescence. Scale bar represents 25 μm.

The *DR5::RFP* reporter showed a more or less complementary pattern (Figure 3A–3D, 3I, and 3J). Although the onset of the DII-YFP-reported auxin response in the valve margin at stage 14 could not be visualized with *DR5::RFP*, we did observe a gradual build-up of auxin response from stages 15–17A, and a clear auxin minimum (Sorefan et al., 2009) in the separation layer of stage 17B fruit (Figures 2F and 3J). Recently it has been shown that the *DR5* reporter in its original guise contains a relatively low affinity binding site for AUXIN RESPONSE FACTORS (Boer et al., 2014; Liao et al., 2015), which might explain the differences between *DR5::GFP/RFP* and *35S::DII-YFP* at stage 14 and also the patchy signal of *DR5::GFP* observed here and elsewhere (Sorefan et al., 2009).

In developing *ind-2* mutant fruits, the picture was much simpler. From stage 13 to stage 17A, the auxin response around the valve margins was low, and only at stage 17B a sudden increase in auxin response was observed in the replum (Figure 3O–3Q). These results are largely in agreement with previous observations using the *DR5::GFP* reporter (Sorefan et al., 2009), except that our more detailed study detected a significant auxin response in the valve margins of wild-type stage 14–17A fruits.

Next we correlated PIN3 expression with the auxin response data. In wild-type fruits, PIN3-GFP was only weakly visible within the replum at stages 11 and 12, but it became more clearly visible at stage 13 (Supplemental Figure 3A–3C), when PIN3-GFP further extended to the valve margin (Figure 3A). PIN3-GFP remained visible in the valve margin of wild-type fruit at stages 14 and 15, when the first cell of the dehiscence zone could be identified, while the abundance in the replum was markedly higher (Figure 3B–3C and Supplemental Figure 3E). A quantification of the PIN3 plasma membrane signal confirmed that PIN3 in the valve margin significantly increased at stage 14 relative to the PIN3 plasma membrane intensity in the replum. At stages 15 and 16, the PIN3-GFP in the dehiscence zone decreased relative

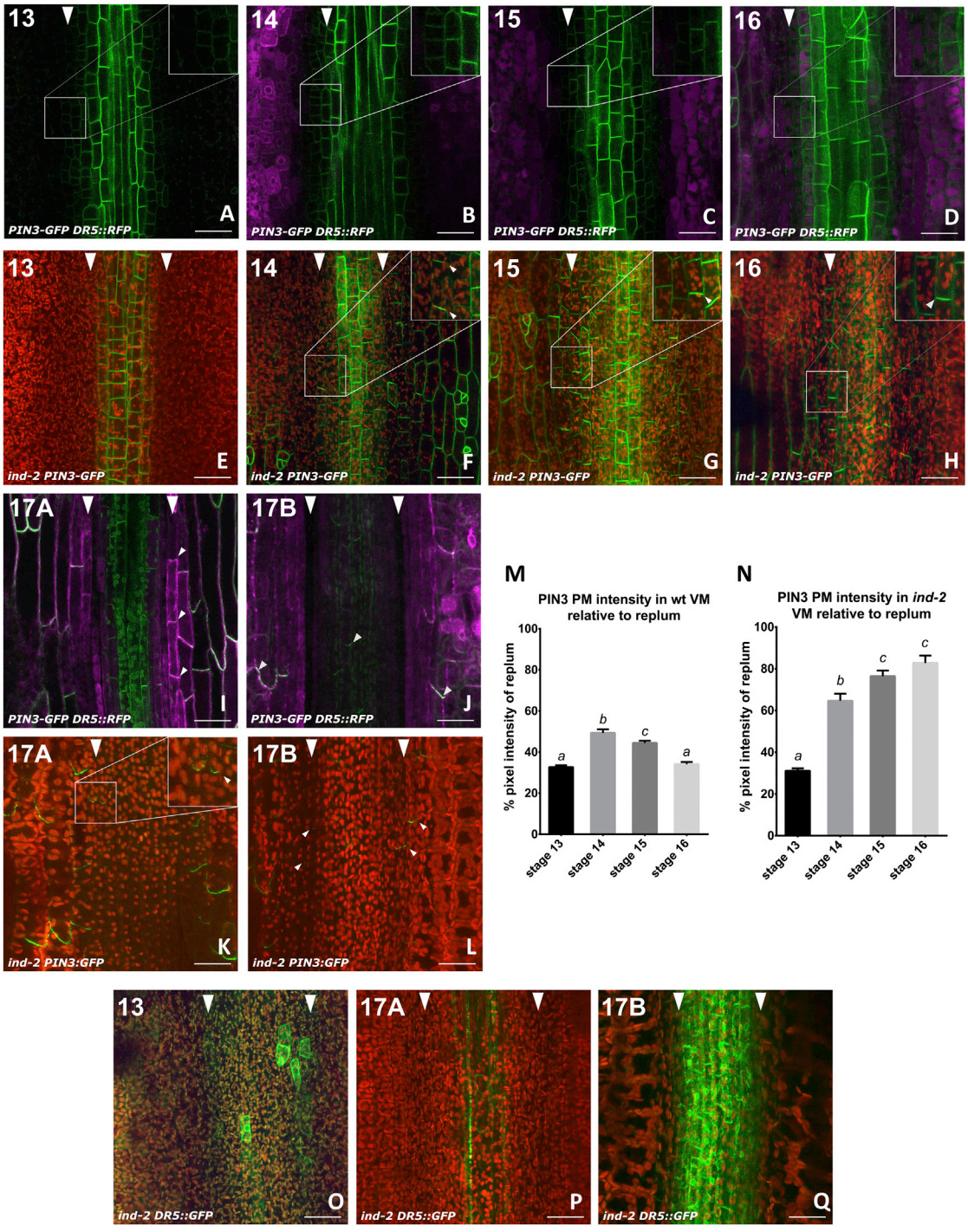

Figure 3. A Transiently Enhanced Auxin Response and PIN3-GFP Plasma Membrane Abundance Coincide with the Establishment of the Separation Layer in Valve Margins of Early *Arabidopsis* Fruit.

(A–L) SUM projection Z stack confocal microscopy images of tangential confocal sections through the epidermal layer of *pin3 PIN3::PIN3-GFP DR5::RFP* **(A–D, I, and J)**, or *ind-2 pin3 PIN3::PIN3-GFP* **(E–H, K, and L)** fruit at stages 13 **(A and E)**, 14 **(B and F)**, 15 **(C and G)**, 16 **(D and H)**, 17A **(I and K)**, and 17B **(J and L)**. Images show PIN3-GFP (green) and RFP (magenta) expression or autofluorescence (red in **E–H, K, and L**) in valves (outer tissues), valve margins (white arrowheads) and replum (inner tissue). The insets in **(A–D, F–H, and K)** show an enlargement of part of the valve margin.

(M and N) Quantification of PIN3-GFP plasma membrane signal in the valve margin relative to replum cells in wild-type **(M)** and *ind-2* **(N)** fruits. Error bars indicate the SE of the mean; bars marked with different letters are significantly different from each other (ANOVA, $p < 0.05$). Per stage, at least eight cells were measured in at least six fruits. All images were collected using the same microscope settings.

(O–Q) SUM projection Z stack confocal microscopy images of tangential confocal sections through the epidermal layer of *ind-2 DR5::GFP* fruit. Images show GFP (green) and autofluorescence (red) in valves (outer tissues), valve margins (white arrowheads), and replum (inner tissue).

The scale bar represents 25 μm.

to the replum (Figure 3D, 3M, and 3N). This decrease continued prior to maturation at stage 17A, resulting in a weak PIN3-GFP signal in the rootward polar domain (Figure 3I), which was still visible at stage 17B (Figure 3J). At stages 17A and 17B, the overall PIN3-GFP abundance appeared reduced. PIN3-GFP was clearly expressed in the epidermis of the valves (Supplemental Figure 3D–3F), but due to the focal plane this was not always visible when focusing on the expression in the dehiscence zone. PIN3-GFP localization and abundance in the *ind-2* mutant appeared similar to that in the wild type up to stage 13 (Figure 3E, 3N, and Supplemental Figure 3C). At stage 14, PIN3-GFP abundance in *ind-2* sharply increased throughout the valve, valve margin, and replum, and this persisted until stage 16 (Figure 3E–3H and Supplemental Figure 3G–3I), and decreased in the same manner as in wild-type stage 17A and B fruits (Figure 3K and 3L). The key difference between the *ind-2* mutant and wild type was that PIN3 abundance in the valve margin increased to 70%–90% of the signal in the replum in stage 14–16 *ind-2* mutant fruits (Figure 3F–3H and 3N), whereas this was significantly lower in wild-type fruits (Figure 3B–3D and 3M).

These data show that in valve margins of wild-type stage 14–16 fruits, an increase in auxin response coincides with a temporary increase in PIN3-GFP abundance. In contrast, no increase in auxin response is observed in stage 14–16 *ind-2* mutant fruits, most likely because of the persistently higher PIN3 plasma membrane abundance in the valve margins of these fruits.

Overexpression of *PID* Leads to Patterning Defects but Not Indehiscence

According to previous data and models, IND represses the expression of *PID* while promoting the expression of *WAG2*, resulting in lateralization of PIN3, thereby generating an auxin minimum in the valve margins of stage 17B fruit (Sorefan et al., 2009; Girin et al., 2011). In line with these data and models, no PID-YFP signal could be detected in the valve margins of developing gynoecia (Girin et al., 2011) or fruits (Supplemental Figure 4), whereas the *WAG2* promoter was shown to be specifically active in valve margins of developing gynoecia (Girin et al., 2011). This implies that *PID* overexpression or *wag2* loss-of-function should result in indehiscent fruits. PID and WAG2 are part of the AGC3 subclade of plant AGCVIII protein serine/threonine kinases in *Arabidopsis*, which includes two other kinase WAG1 and AGC3-4 (Galván-Ampudia and Offringa, 2007). Previously, it was shown that PID, WAG1, and WAG2 are functionally redundant (Cheng et al., 2008; Dhonukshe et al., 2010). Strong *pid* alleles are unable to produce fruits, thus we investigated dehiscence zone formation in *wag2* single and *wag1 wag2* double loss-of-function mutants. Close examination of the mature fruit of both mutants showed that dehiscence zone formation was not affected (Figure 4F–4I) and that fruits were able to open normally upon dehiscence (Figure 4A–4C), whereas *ind-2* mutant fruits did not (Figure 4B and 4G). The local auxin minimum observed in the separation layer of mature wild-type fruits was also detected in both mutant backgrounds providing further evidence that dehiscence zone formation is undisturbed in these mutants (Figure 4K and 4L). Examination of fruits developing on *35S::PID* plants revealed severe defects in valve patterning in some fruits (Figure 4M–4O). Valves initiated asymmetrically along the replum, resulting in fused repla at the base (Figure 4N). However, normal valve patterning was restored in the more apical parts of the fruit. Although tissue patterning was partially disturbed, scanning electron microscopy (SEM) imaging and transverse sections showed that dehiscence zone formation occurred (Figure 4J and 4O), and fruits indeed opened normally upon dehiscence (Figure 4E). These results show that simply upregulating or knocking down the expression of *PID* or *WAG2* is not sufficient to disrupt the patterning of the valve margin region.

Valve Margin-Specific Expression of *PID* and *WAG2* Results in Indehiscence

Our analysis of *PID* expression in *pid PID::PID-YFP* fruits (Supplemental Figure 4) suggested that *PID* is specifically repressed in the valve margin as early as stage 13, and according to the model (Girin et al., 2011), *WAG2* is upregulated during valve margin specification. *IND* promoter-driven *GUS* expression is valve margin-specific and strong during gynoecium development (stages 11 and 12), while it is expressed in the same tissues but weaker during fruit development (stages 14–17) (Sorefan et al., 2009). This suggests that valve margin-specific expression of *PID* or *WAG2* under the *IND* promoter would respectively repress or promote dehiscence zone specification. However, introduction of either *IND::WAG2-RFP* or *IND::PID-RFP* in the *ind-2* mutant background could not rescue the *ind* phenotype. Transverse fruit sections did not show dehiscence zone cell specification, and upon fruit maturation, no valve separation was observed (Figure 5F and 5G). Unexpectedly, introduction of either *IND::PID* or *IND::WAG2* expression in wild-type background resulted in indehiscent fruit in 20% (n = 21) and 30% (n = 26) of the transformants, respectively. The phenotype of single insert transgenic indehiscent lines transmitted to the next generation and was fully penetrant. Semi-quantitative RT–PCR on RNA isolated from stage 13–17 indehiscent fruits confirmed that *IND* itself was not silenced (Supplemental Figure 5A), and that, in the *IND::PID* transgenic lines, *PID-RFP* was ectopically expressed (Supplemental Figure 5B). It has to be noted here that the *IND* transcript could still be detected in the *ind-2* mutant, since this allele has a frameshift mutation that causes an early stop in translation, which does not affect transcription (Liljegren et al., 2004). Transverse sections of the *IND::PID* and *IND::WAG2* transformants showed that they mimicked the *ind-2* phenotype, and that they lacked the sutures between the replum and valves that are characteristic for the valve margin and dehiscence zone (Figure 5A–5D). Valve margin-specific expression of *WAG1* or *AGC3-4* did not result in indehiscent fruit in 24 T1 plants (Figure 5E), indicating that the indehiscent phenotype is specific for the PID and WAG2 kinases, and corroborating that the phenotype is not merely caused by silencing of the *IND* gene through the introduction of one or more extra copies of the *IND* promoter. Our results on the valve margin-specific expression of *PID* and *WAG2* suggest that both *PID* and *WAG2* expression needs to be repressed by IND during dehiscence zone specification.

Valve Margin-Specific Expression of PID and WAG2 Leads to an Increase in PIN3-GFP in the Valve Margin

Our previous observations suggested that IND repression of *PID* (and according to our data also of *WAG2*) in the valve

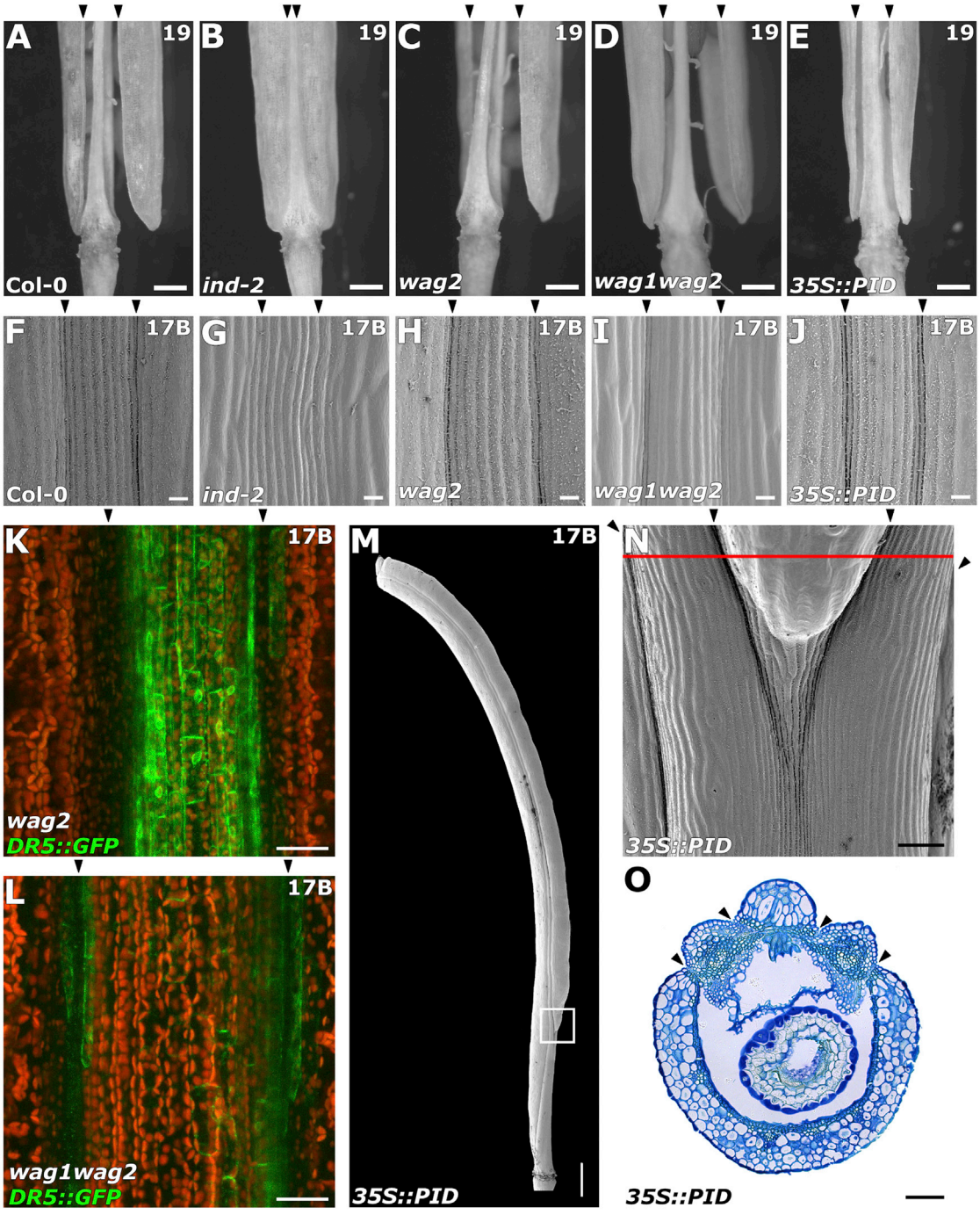

Figure 4. *wag1 wag2* Loss of Function or *35S::PID* Do Not Affect Dehiscence Zone Formation.

(A–E) Images of the lower part of completely dried wild-type **(A)**, *ind-2* **(B)**, *wag2* **(C)**, *wag1wag2* **(D)**, *35S::PID* **(E)** fruit at the moment of valve separation. Black arrowheads indicate the position of the dehiscence zone.

(F–J) Scanning electron micrographs of the valve margins (black arrowheads) of wild-type **(F)**, *ind-2* **(G)**, *wag2* **(H)**, *wag1wag2* **(I)**, and *35S::PID* **(J)** fruit.

(K and L) Tangential confocal images through the epidermis of stage 17B *DR5::*GFP *wag2* or *DR5::*GFP *wag1 wag2* fruit, showing an auxin response minimum in the separation layer (black arrowheads).

(M–O) Valve patterning defects in stage 17B *35S::PID* fruits as observed by scanning electron microscopy (**(N)** shows a detailed view of the boxed area in **(M)**), or in a transverse toluidine blue-stained section **(O)** at the height of unequal valve separation, as indicated by the red line in **(N)**. Black arrowheads indicate the positions of the valve margins.

Scale bar represents 100 μm in **(A–E)**, 10 μm in **(F–J)**, 25 μm in **(K–L)**, and 50 μm in **(M–O)**.

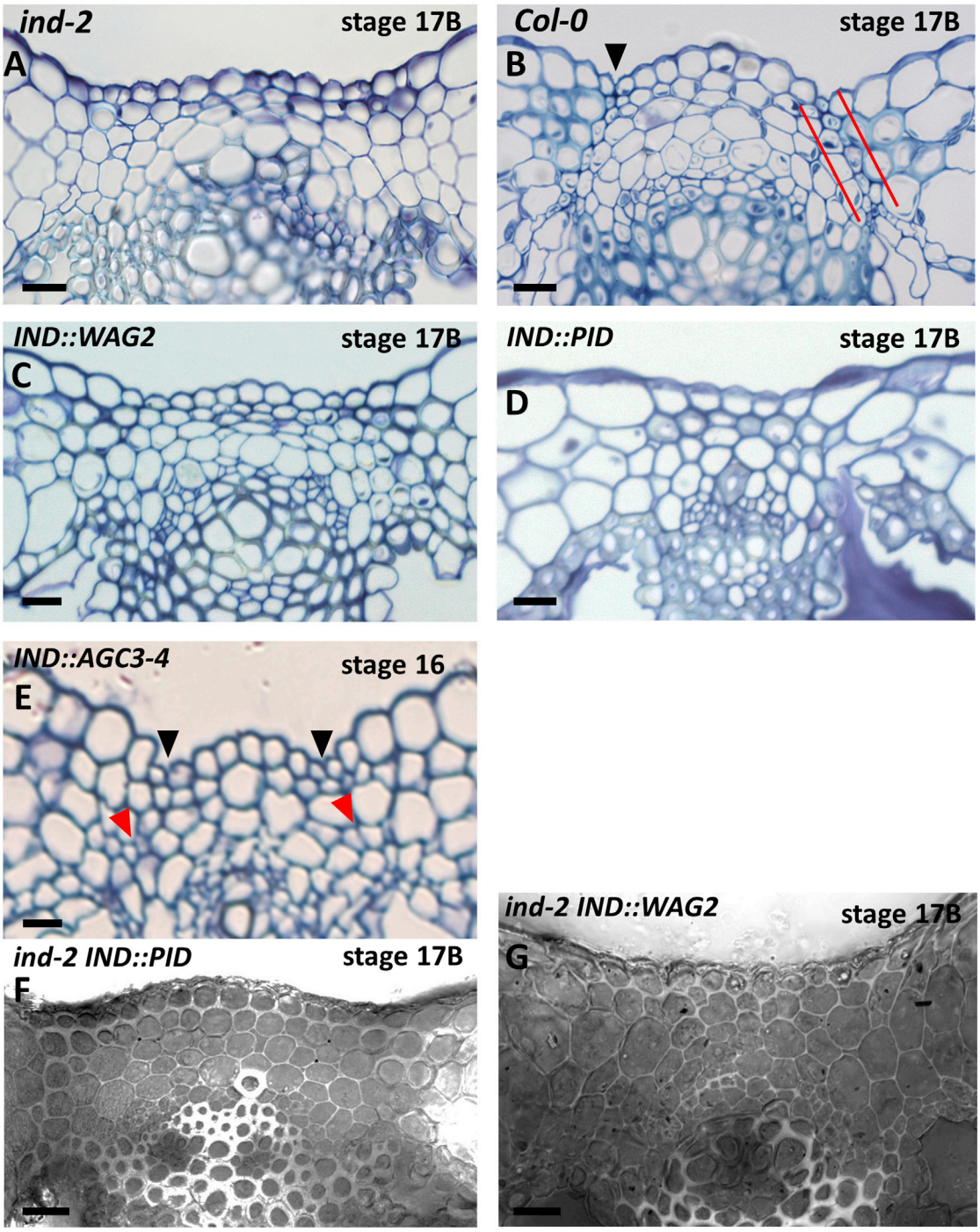

Figure 5. *IND::PID* and *IND::WAG2* Mimic *ind* Loss of Function.

(A–G) Images of median transversal sections of *ind-2* **(A)**, wild-type **(B)**, *IND::WAG2* **(C)**, *IND::PID* **(D)**, *IND::AGC3-4* **(E)**, *ind-2 IND::PID* **(F)**, *ind-2 IND::WAG2* **(G)** fruit. **(A–E)** are stained with toluidine blue, while **(F and G)** are not. The black arrowheads in **B** and **E** indicate the sutures formed during SL development, and the red arrowheads in **E** point out formative cell divisions during SL development. The red lines in **B** mark de smaller, stronger stained cells in the SL. The scale bar shows corresponding sizes throughout the images. Scale bar represents 10 μM.

margins of 14–16 stage fruits is required to reduce PIN3-GFP abundance, allowing an increase in auxin response that is crucial during these stages for dehiscence zone specification. PIN3-GFP levels were indeed significantly higher in the valve margins of stage 16 *ind-2* mutant fruit, where it showed a more predominant rootward/shootward polar localization compared with wild-type fruit (Figures 3F–3H, 6A, and 6B). *IND::PID* and *IND::WAG2* fruit showed similar enhanced PIN3-GFP levels in the valve margins (Figure 6C and 6D, quantified in 6E), compared with wild-type fruit (Figure 6A), and these enhanced levels correlated with a reduced expression of the *DR5::GFP* auxin response reporter (Figure 6F–6H). Our results are in line

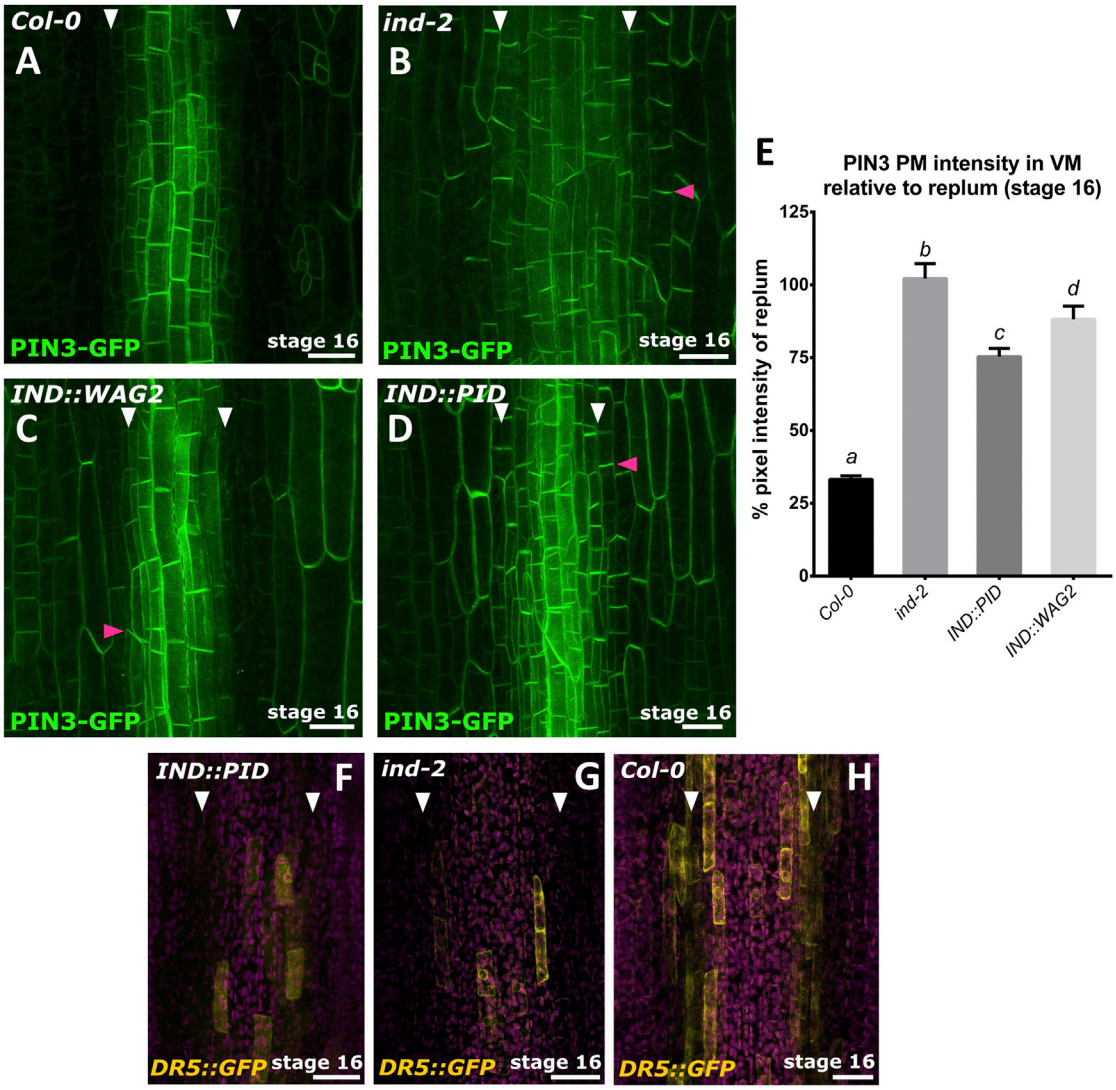

Figure 6. *IND::PID* and *IND::WAG2* Show an Enhancement in PIN3-GFP Abundance.
(A–H) Confocal microscopy images of wild-type **(G)**, *ind-2* **(F)**, *IND::PID* **(D and E)**, and *IND::WAG2* **(C)**, expressing *PIN3-GFP* (green) (**A–D**, quantified in **E**) or *DR5::GFP* (yellow) **(F–H)**, showing the valves, valve margin (white arrowheads), and replum at stage 16. Images were taken at the median region of the fruit. Z stack images were projected to yield the final pictures and the magenta signal depicts the autofluorescence signal (>650 nm). The scale bar represents 20 μm. Quantification of plasma membrane PIN3-GFP abundance was performed in the same manner as in Figure 3. The pink arrowheads point towards polarized PIN3-GFP plasma membrane signal. Error bars indicate the SE of the mean; bars marked with different letters are significantly different from each other (ANOVA, $p < 0.05$).

with a model that dehiscence zone specification occurs at stage 14–16 of fruit development, and that, at these stages, an elevated auxin response rather than an auxin minimum is required for dehiscence zone specification, which is attained by IND-mediated repression of PID and WAG2 kinase expression.

DISCUSSION

The IND transcription factor determines the opening of *Arabidopsis* fruits by specifying the dehiscence zone in the valve margin between the valve and replum (Liljegren et al., 2004). Previous research has led to the model that IND dimerizes with SPT to bind the *PID* and *WAG2* promoters, leading to repression of *PID* expression and upregulation of *WAG2*. This in turn enhances the plasma membrane abundance of PIN3, causing an auxin minimum in the dehiscence zone of stage 17B fruit, which is needed to specify the separation layer (Sorefan et al., 2009; Ding et al., 2011; Girin et al., 2011). While investigating the antagonistic function of PID and WAG2 in this developmental process, we looked more in detail into the timing of events during dehiscence zone specification. Our data show that the cell divisions that create the separation layer in the valve margin firstly occur just after pollination in stage 14 fruit (for model, see Figure 7). Interestingly, the start of these divisions coincided with an increase of auxin in the valve margin, which is different from the requirement for an auxin minimum later in fruit development to initiate separation (Sorefan et al., 2009). The auxin levels in the developing dehiscence zone increase until stage 15 and lower slightly toward stage 17A, followed by the rapid formation of an auxin

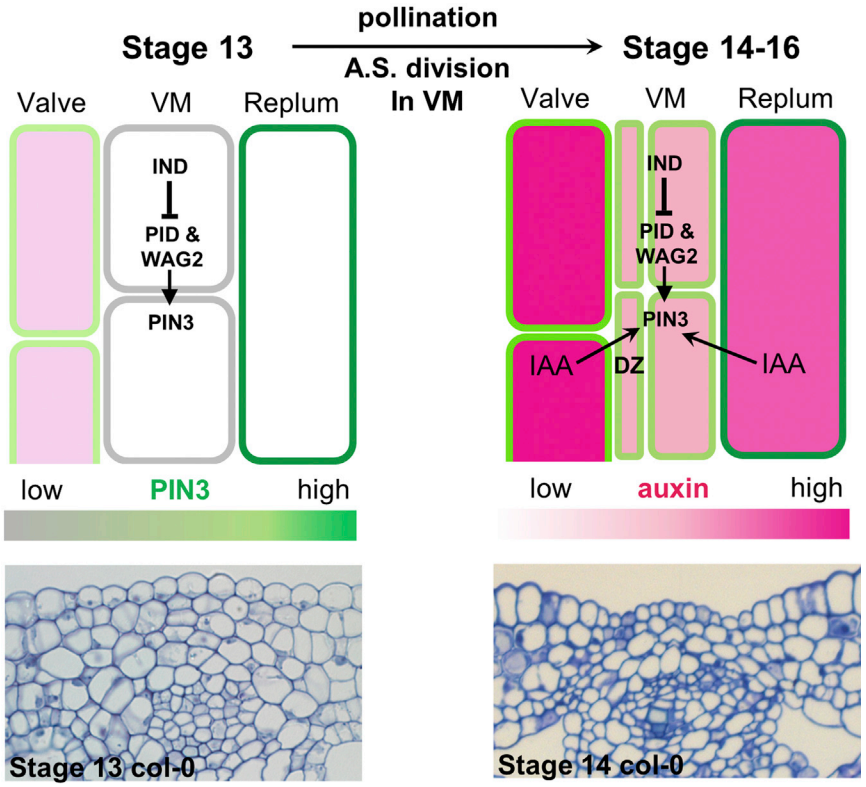

Figure 7. IND Specifies the Dehiscence Zone in Stage 14–16 Fruit by Repressing *PID* and *WAG2* Expression.

Model depicting the transition toward dehiscence zone (DZ) specification. Auxin levels are depicted in a pink fill, while PIN3-GFP plasma membrane levels are depicted in a green outline. Pollination takes place at stage 13 and fertilization at stage 14. PIN3 at stage 13 is present in the replum and somewhat in the valves. IND represses *PID* and *WAG2*, thereby decreasing PIN3 plasma membrane abundance. At stage 14, the developing ovules cause an influx of auxin through the replum, while the biosynthesis of auxin in the valves increases as well. This increase in auxin in the valves and replum causes an auxin influx into the valve margin, which has a net auxin influx due to the relatively low PIN3 plasma membrane abundance. Auxin itself promotes PIN3 at the plasma membrane through inhibition of endocytosis (Paciorek et al., 2005), creating subsequent auxin efflux. This results in a medium amount of auxin, which is beneficial for the asymmetric (A.S.) divisions specifying the dehiscence zone (DZ).

minimum in the separation layer of the mature fruit. We propose that both *PID* and *WAG2* are repressed by IND, which is strongly expressed during early fruit development, and that this lowers PIN3 levels relative to the replum, resulting in a net influx of auxin into the valve margin at stages 14–16 (Figure 7). The amount of auxin available increases at those stages (Sorefan et al., 2009), which could be due to increased local auxin biosynthesis by *TAA1* or *YUCCA 2*, for which the expression is detectable in the relevant regions and stages (Cheng et al., 2006; Trigueros et al., 2009; Martínez-Fernández et al., 2014). Another possibility is that the developing ovules, which are known to promote fruit growth (Dorcey et al., 2009; Fuentes et al., 2012), would be the source of auxin. Arguing against this is the observation that the female-sterile *es1-D* mutant does produce a fruit without ovules that shows normal dehiscence (Sotelo-Silveira et al., 2013).

The increase in auxin levels in turn promotes PIN3 plasma membrane abundance (Paciorek et al., 2005), causing auxin efflux and the subsequent drop in PIN3 abundance from stage 15 onward. The true auxin minimum occurs only at the end of dehiscence zone formation (stage 17B) and may therefore mediate the final cell dissolution rather than separation layer differentiation. Our model explains why valve margin-specific expression of *PID* and *WAG2* induces indehiscence. Expression of these kinases stimulates the plasma membrane abundance of PIN3, thereby preventing the moderate increase in auxin levels that induces the cell divisions leading to separation layer formation.

This model predicts that an elevated auxin response during early fruit development is necessary for separation layer specification, whereas *IND* promoter-driven expression of the bacterial auxin biosynthesis gene *iaaM* suggested that elevated auxin levels result in an indehiscent phenotype (Sorefan et al., 2009). Most likely the timing and the level of the auxin response are important here. In stage 13 fruit, auxin responses are low and in stage 14–16 fruits only a moderately elevated auxin response was observed in the valve margin (Figures 2 and 3). The auxin levels and responses induced by *IND::iaaM* expression are probably too high for these early stages of fruit development, and thus inhibit the cell division and differentiation processes that are required to specify the dehiscence zone.

Cytokinin (BA) application to the gynoecium 24 h after pollination has been shown to rescue *ind-2* and *shatterproof1 shatterproof2* (*shp1 shp2*) double mutant phenotypes (Marsch-Martínez et al., 2012). BA treatment has also been shown to remove PIN1 from the anticlinal membranes of lateral root primordia cells. In the latter case, evidence was provided that BA acts by repressing PID activity (Marhavý et al., 2014). Possibly, BA also has a direct effect on PID in the developing *ind-2* and *shp* fruits, which would mimic the repression by IND in the wild-type. BA might thus remove PIN3 from the plasma membrane of VM cells by decreasing PID activity and thereby creating an auxin sink in the valve margin region.

Our model differs from the earlier reported model where IND and SPT upregulate the expression of *WAG2* and repress the expression of *PID* (Sorefan et al., 2009; Girin et al., 2011). The indehiscence caused by ectopic valve margin-specific expression of *WAG2* suggests that general downregulation of AGC3 kinase activity is necessary for separation layer specification. The previously reported differential regulation of *PID* and *WAG2* is based on qRT–PCR analysis on RNA extracted from 7-day-old

DEX-induced *35S::IND-GR* seedlings or from whole wild-type, *ind*-2, and *ful* (*IND* overexpression) mutant stage 15 fruits (Sorefan et al., 2009). However, based on the analysis of *PID::PID-VENUS* (Supplemental Figure 4) and *pWAG2-GUS* (Girin et al., 2011) reporter lines, both genes are not expressed in the valve margins after anthesis. For *WAG2*, this result is surprising, since IND is expressed in developing fruit up to stage 17, and thus one would expect the *WAG2* promoter to be active during these stages. This suggests that *WAG2*, although reported to be activated by ectopically expressed IND, does not play a role in dehiscence zone specification. More cell-type-specific methods, such as laser microdissection, could be used to verify the effects of IND and SPT on *PID* and *WAG2* expression in the dehiscence zone at RNA level. Our results suggest that repression of AGC3 kinase expression is essential to reduce PIN3-GFP abundance for separation layer specification. Although we cannot exclude that *IND* promoter-driven misexpression of *PID* and *WAG2*, like for the *iaaM* gene, has yet unforeseen effects on auxin dynamics during crucial developmental stages, our results are in line with a redundant (Dhonukshe et al., 2010) rather than a differential developmental role for these two kinases. The fact that we do not observe indehiscence with *IND* promoter controlled *WAG1* or *AGC3-4* expression suggests that the four AGC3 kinases do not necessarily show redundant functionality when ectopically expressed.

Differential plasma membrane abundance of PIN3-GFP and the resulting auxin levels are known to be crucial in modulating cell divisions during stomatal development. Here auxin depletion, coinciding with reduced PIN3-GFP abundance, triggers a developmental switch allowing the symmetric division of the guard mother cell that generates the two guard cells (Le et al., 2014). An auxin minimum and reduced PIN3-GFP abundance were also observed in the dehiscence zone in stage 17B fruit, but there is no evidence that the minimum triggers symmetric cell divisions. The auxin minimum at stage 17B may thus be of an instructive nature and act as a final cue in specifying the cell fate of the separation layer (Figure 7). This process could be regulated by ALC (Rajani and Sundaresan, 2001), since *alc* loss-of-function mutant fruits develop a dehiscence zone with characteristic sutures but remain indehiscent.

In contrast to the final symmetric cell division that forms the stoma, the cell divisions that generate the dehiscence zone in stage 14–16 fruits seem asymmetric, as transverse sections through developing fruit suggest that smaller cells are formed from the larger cells in the developing valve margin (Figure 1). Due to the tapered nature of these separation layer cells, it is difficult to determine their exact shape and size, and 3D time-lapse imaging would be needed to resolve this issue. Still, asymmetry of the cell divisions generating the separation layer would be more in line with their formative nature, and with our observations that a mild elevation in auxin response, rather than auxin depletion, occurs in the valve margin of stage 14–16 fruits.

In conclusion, we propose that IND facilitates the early specification of the dehiscence zone, which is missing in *ind-2* fruit, by repressing AGC3 kinase activity, thereby precisely controlling the auxin levels in the dehiscence zone through PIN3-mediated auxin efflux and instructing formation of the separation layer.

METHODS

Plant Lines and Plant Growth

All *Arabidopsis* lines are in the Col-0 background. The *wag1* (SALK_002056), *wag2* (SALK_070240) mutant alleles (Santner and Watson, 2006), and the transgenic lines *PID::PID-VENUS:* (Michniewicz et al., 2007), *35S::DII-YFP* and *35S::mDII-YFP* (Brunoud et al., 2012), *ind-2 DR5::GFP* and *ind-2 PIN3-GFP* (Sorefan et al., 2009) have been previously described. *wag2 DR5::GFP* and *wag1wag2 DR5::GFP* plants were selected from earlier described *wag2 pid14+/− DR5::GFP* and *wag1wag2 pid14+/− DR5::GFP* lines (Dhonukshe et al., 2010). The *pin3 PIN3::PIN3-GFP DR5::RFP* line was obtained by crossing the previously described *pin3 PIN3::PIN3-GFP* line (Friml et al., 2002) with the *DR5::RFP* line (Marhavý et al., 2011). Primers for genotyping are listed in Supplemental Table 1 (primers 1–3). All plants were grown under long-day conditions (16/8 h light/dark), at 21°C and 70% relative humidity.

Molecular Cloning

The *IND* promoter was PCR amplified from the *IND::IND-GUS* template plasmid (Sorefan et al., 2009) using primer pair 12 and 13 (Supplemental Table 1). The *IND* promoter fragment was cloned into the *Asc*I digested pGreenII-based gateway *tagRFP* containing vector, upstream of the Gateway cassette and the *tagRFP* gene. The *PID*, *WAG2* and *AGC3-4* coding sequences were Gateway recombined into this destination vector, generating the final *IND::PID* (or *WAG2*/*AGC3-4*)-*tagRFP* constructs. All primer sequences used for the molecular cloning are described in (Dhonukshe et al., 2010) for *PID* and *WAG2* or listed in Supplemental Table 1.

Plant Transformation and Selection

The constructs *IND::PID-tagRFP*, *IND::WAG2-tagRFP* and *IND::AGC3-4-tagRFP* were introduced into *Agrobacterium* strain AGL1 by electroporation and transgenic *Arabidopsis* lines were obtained by floral dip transformation (Davis et al., 2009). Primary transformants were selected using 30 μg/ml phosphinothricin (PPT; Duchefa) and single locus homozygous T2 plants were selected on 30 μg/ml PPT and transferred to soil to be assessed for separation layer defects, either by assessing fruit opening upon complete maturation of the fruit, or by investigating separation layer formation in transverse hand sections of the middle of stage 17B fruits.

RNA Isolation and RT–PCR

Staged gynoecia and fruits were ground and used for an RNA extraction using a Nucleospin RNA kit (Machery-Nagel). The resulting RNA was used in a first-strand synthesis reaction with M-MLV reverse transcriptase (according to the manual; Promega) and the resulting cDNA was used as a template for a semi-quantitative RT–PCR reaction with 29 cycles to amplify products of either *IND* (primers 10 and 11), *tagRFP* (primers 8 and 9) or of the *UBQ10* reference gene (primers 14 and 15) (Supplemental Table 1).

Microscopy and Embedding

All samples for embedding and SEM were fixed overnight in 2% paraformaldehyde and 1% glutaraldehyde in 1× phosphate buffered saline (PBS, pH7). Fixed samples were subsequently dehydrated in an increasing range of alcohol (for embedding) or acetone (for SEM). For embedding, the middle 5 mm of the fruit was incubated in propylene oxide for 2 × 15 min at room temperature, then transferred to a 1:1 mixture of propylene oxide and Epon for 2 h at room temperature. Fresh Epon was added and samples were incubated overnight and placed in silicon molds the following day. Polymerization of the Epon was conducted at 60°C for 2 days. Histological sections were prepared using a Leica RM 2165 rotary microtome, in combination with handmade glass knives. Sections were made in the range of 2–3 μm and placed in water, then heat-fixed to the object glass using a hot plate. Sections were stained with 0.1% toluidine blue solution for 1 min, rinsed with demineralized water, and dried at 37°C for 2 days. Sections were mounted in Epon and polymerization was done

at 60°C overnight. Images were obtained using the Zeiss Axioplan 2 microscope, equipped with a Zeiss AxioCam MRc 5 digital color camera.

After acetone dehydration, SEM samples were dried using the Bal-Tec CDP030 critical point dryer and samples were fixed to stubs to be coated with gold using the SEM Coating Unit 5100 (Polaron Equipment). Samples were viewed using the JEOL SEM 6400 scanning electron microscope.

Confocal microscopy was performed using either an inverted Zeiss LSM5 Exciter/AxioObserver or an upright Zeiss LSM5 Exciter/AxioImager confocal laser scanning microscope. Whole-mount fruits were viewed immediately after collection, using a 40× long working distance water immersion objective. The following lasers and bandpass filters were used: GFP, 488 nm laser, 505–530 nm filter; YFP, 514 nm laser, 530–560 nm filter; RFP, 543 nm laser; autofluorescence was captured with a 650 nm long-pass filter. Confocal microscope settings were kept identical between developmental stages and genotypes. To reduce water tension, samples were first washed in a 1% Tween solution, rinsed thoroughly with demineralized water, and fixed to object glasses using superglue. Autofluorescence was detected using a 650 nm long-pass filter. All images were processed using ImageJ, ICY (http://icy.bioimageanalysis.org/), GIMP (http://www.gimp.org), or Adobe Photoshop CS5 (http://www.adobe.com).

Quantification of PIN3-GFP

For the quantification of PIN3-GFP abundance, the entire plasma membrane signal of nine cells in either the valve margin or the replum was measured using single optical sections (where the valve margin was visible) derived from Z stack images of the valve margin/replum/valve region (Figure 3). Per stage images of seven to eight independent fruits were analyzed. For each cell, the average pixel intensity value of the GFP channel was used to calculate an average value per stage/cell type, and the valve margin values were then divided by the average replum values. All measurements were performed with the area tool of ICY (http://icy.bioimageanalysis.org/).

(m)DII-YFP Microscopy and Intensity Measurements

Z stacks of 30.13 μm of the valve margins of *DII-YFP* and *mDII-YFP* fruits were taken using a Leica SP8 confocal microscope (http://www.leica-microsystems.com). Samples were excited using a 514 nm solid-state laser, and settings were kept identical between different developmental stages within each line. The YFP intensity levels were determined by summing the Z stacks and measuring the average fluorescence levels within a rectangle covering the valve margin area, using Fiji (http://fiji.sc). One valve margin of eight individual fruits was measured per developmental stage.

SUPPLEMENTAL INFORMATION

Supplemental Information is available at *Molecular Plant Online*.

FUNDING

K.v.G. was supported by an NWO-CW TOP grant (700.58.301) to R.O. from the Chemical Sciences Division with financial support from the Netherlands Organisation for Scientific Research (NWO).

AUTHOR CONTRIBUTIONS

K.v.G., M.v.R., and R.O. designed the experiments and wrote the paper. K.v.G., M.v.R., A.L., and A.O. performed experiments.

ACKNOWLEDGMENTS

We would like to thank Lars Østergaard for providing various reporter lines in wild-type and *ind-2* mutant background and the *IND* promoter clones; Eva Benkova for providing the *DR5::RFP* line. Moreover, we are grateful to Lars Østergaard and to Emma Larsson for their critical comments on the manuscript. No conflict of interest declared.

Received: November 11, 2015
Revised: March 4, 2016
Accepted: March 9, 2016
Published: March 16, 2016

REFERENCES

Benjamins, R., Quint, A., Weijers, D., Hooykaas, P., and Offringa, R. (2001). The PINOID protein kinase regulates organ development in *Arabidopsis* by enhancing polar auxin transport. Development **128**:4057–4067.

Benková, E., Michniewicz, M., Sauer, M., Teichmann, T., Seifertová, D., Jürgens, G., and Friml, J. (2003). Local, efflux-dependent auxin gradients as a common module for plant organ formation. Cell **115**:591–602.

Boer, D.R., Freire-Rios, A., van den Berg, W.A., Saaki, T., Manfield, I.W., Kepinski, S., López-Vidrieo, I., Franco-Zorrilla, J.M., de Vries, S.C., Solano, R., et al. (2014). Structural basis for DNA binding specificity by the auxin-dependent ARF transcription factors. Cell **156**:577–589.

Brunoud, G., Wells, D.M., Oliva, M., Larrieu, A., Mirabet, V., Burrow, A.H., Beeckman, T., Kepinski, S., Traas, J., Bennett, M.J., et al. (2012). A novel sensor to map auxin response and distribution at high spatio-temporal resolution. Nature **482**:103–106.

Cheng, Y., Dai, X., and Zhao, Y. (2006). Auxin biosynthesis by the YUCCA flavin monooxygenases controls the formation of floral organs and vascular tissues in *Arabidopsis*. Genes Dev. **20**:1790–1799.

Cheng, Y., Qin, G., Dai, X., and Zhao, Y. (2008). NPY genes and AGC kinases define two key steps in auxin-mediated organogenesis in *Arabidopsis*. Proc. Natl. Acad. Sci. USA **105**:21017–21022.

Davis, A.M., Hall, A., Millar, A.J., Darrah, C., and Davis, S.J. (2009). Protocol: streamlined sub-protocols for floral-dip transformation and selection of transformants in *Arabidopsis thaliana*. Plant Methods **5**:3.

Dhonukshe, P., Huang, F., Galvan-Ampudia, C.S., Mähönen, A.P., Kleine-Vehn, J., Xu, J., Quint, A., Prasad, K., Friml, J., Scheres, B., et al. (2010). Plasma membrane-bound AGC3 kinases phosphorylate PIN auxin carriers at TPRXS(N/S) motifs to direct apical PIN recycling. Development **137**:3245–3255.

De Smet, I., and Beeckman, T. (2011). Asymmetric cell division in land plants and algae: the driving force for differentiation. Nat. Rev. Mol. Cell Biol. **12**:177–188.

Ding, Z., Galván-Ampudia, C.S., Demarsy, E., Łangowski, Ł., Kleine-Vehn, J., Fan, Y., Morita, M.T., Tasaka, M., Fankhauser, C., Offringa, R., et al. (2011). Light-mediated polarization of the PIN3 auxin transporter for the phototropic response in *Arabidopsis*. Nat. Cell Biol. **13**:447–452.

Dorcey, E., Urbez, C., Blázquez, M.A., Carbonell, J., and Perez-Amador, M.A. (2009). Fertilization-dependent auxin response in ovules triggers fruit development through the modulation of gibberellin metabolism in *Arabidopsis*. Plant J. **58**:318–332.

Ferrándiz, C. (2002). Regulation of fruit dehiscence in *Arabidopsis*. J. Exp. Bot. **53**:2031–2038.

Ferrándiz, C., Pelaz, S., and Yanofsky, M.F. (1999). Control of carpel and fruit development in *Arabidopsis*. Annu. Rev. Biochem. **68**: 321–354.

Ferrándiz, C., Liljegren, S.J., and Yanofsky, M.F. (2000). Negative regulation of the SHATTERPROOF genes by FRUITFULL during *Arabidopsis* fruit development. Science **289**:436–438.

Friml, J., Wiśniewska, J., Benková, E., Mendgen, K., and Palme, K. (2002). Lateral relocation of auxin efflux regulator PIN3 mediates tropism in *Arabidopsis*. Nature **415**:806–809.

Friml, J., Yang, X., Michniewicz, M., Weijers, D., Quint, A., Tietz, O., Benjamins, R., Ouwerkerk, P.B., Ljung, K., Sandberg, G., et al.

(2004). A PINOID-dependent binary switch in apical-basal PIN polar targeting directs auxin efflux. Science **306**:862–865.

Fuentes, S., Ljung, K., Sorefan, K., Alvey, E., Harberd, N.P., and Ŕstergaard, L. (2012). Fruit growth in *Arabidopsis* occurs via DELLA-dependent and DELLA-independent gibberellin responses. Plant Cell **24**:3982–3996.

Galván-Ampudia, C.S., and Offringa, R. (2007). Plant evolution: AGC kinases tell the auxin tale. Trends Plant Sci. **12**:541–547.

Girin, T., Paicu, T., Stephenson, P., Fuentes, S., Körner, E., O'Brien, M., Sorefan, K., Wood, T.A., Balanzá, V., Ferrándiz, C., et al. (2011). INDEHISCENT and SPATULA interact to specify carpel and valve margin tissue and thus promote seed dispersal in *Arabidopsis*. Plant Cell **23**:1–14.

Le, J., Liu, X.-G., Yang, K.-Z., Chen, X.L., Zou, J.J., Wang, H.Z., Wang, M., Vanneste, S., Morita, M., Tasaka, M., et al. (2014). Auxin transport and activity regulate stomatal patterning and development. Nat. Commun. **5**:3090.

Liao, C., Smet, W., Brunoud, G., Yoshida, S., Vernoux, T., and Weijers, D. (2015). Reporters for sensitive and quantitative measurement of auxin response. Nat. Methods **12**:207–210.

Liljegren, S.J., Roeder, A.H.K., Kempin, S.A., Gremski, K., Ŕstergaard, L., Guimil, S., Reyes, D.K., and Yanofsky, M.F. (2004). Control of fruit patterning in *Arabidopsis* by INDEHISCENT. Cell **116**:843–853.

Marhavý, P., Bielach, A., Abas, L., Abuzeineh, A., Duclercq, J., Tanaka, H., Pařezová, M., Petrášek, J., Friml, J., Kleine-Vehn, J., et al. (2011). Cytokinin modulates endocytic trafficking of PIN1 auxin efflux carrier to control plant organogenesis. Dev. Cell **21**:796–804.

Marhavý, P., Duclercq, J., Weller, B., Feraru, E., Bielach, A., Offringa, R., Friml, J., Schwechheimer, C., Murphy, A., and Benková, E. (2014). Cytokinin controls polarity of PIN1-dependent auxin transport during lateral root organogenesis. Curr. Biol. **24**:1031–1037.

Marsch-Martínez, N., Ramos-Cruz, D., Reyes-Olalde, J.I., Lozano-Sotomayor, P., Zúñiga-Mayo, V.M., and de Folter, S. (2012). The role of cytokinin during *Arabidopsis* gynoecia and fruit morphogenesis and patterning. Plant J. **72**:222–234.

Martínez-Fernández, I., Sanchís, S., Marini, N., Balanzá, V., Ballester, P., Navarrete-Gómez, M., Oliveira, A.C., Colombo, L., and Ferrándiz, C. (2014). The effect of NGATHA altered activity on auxin signaling pathways within the *Arabidopsis* gynoecium. Front. Plant Sci. **5**:210.

Michniewicz, M., Zago, M.K., Abas, L., Weijers, D., Schweighofer, A., Meskiene, I., Heisler, M.G., Ohno, C., Zhang, J., Huang, F., et al. (2007). Antagonistic regulation of PIN phosphorylation by PP2A and PINOID directs auxin flux. Cell **130**:1044–1056.

Østergaard, L. (2009). Don't"leaf" now. The making of a fruit. Curr.Opin.Plant Biol. **12**:36–41.

Paciorek, T., Zazímalová, E., Ruthardt, N., Petrásek, J., Stierhof, Y.D., Kleine-Vehn, J., Morris, D.A., Emans, N., Jürgens, G., Geldner, N., et al. (2005). Auxin inhibits endocytosis and promotes its own efflux from cells. Nature **435**:1251–1256.

Rajani, S., and Sundaresan, V. (2001). The *Arabidopsis* myc/bHLH gene alcatraz enables cell separation in fruit dehiscence. Curr. Biol. **11**:1914–1922.

Roeder, A.H.K., Ferrándiz, C., and Yanofsky, M.F. (2003). The role of the REPLUMLESS homeodomain protein in patterning the *Arabidopsis* fruit. Curr. Biol. **13**:1630–1635.

Santner, A.A., and Watson, J.C. (2006). The WAG1 and WAG2 protein kinases negatively regulate root waving in *Arabidopsis*. Plant J. **45**:752–764.

Smyth, D.R., Bowman, J.L., and Meyerowitz, E.M. (1990). Early flower development in *Arabidopsis*. Plant Cell **2**:755–767.

Sorefan, K., Girin, T., Liljegren, S.J., Ljung, K., Robles, P., Galván-Ampudia, C.S., Offringa, R., Friml, J., Yanofsky, M.F., and Østergaard, L. (2009). A regulated auxin minimum is required for seed dispersal in *Arabidopsis*. Nature **459**:583–586.

Sotelo-Silveira, M., Cucinotta, M., Chauvin, A.-L., Chávez Montes, R.A., Colombo, L., Marsch-Martínez, N., and de Folter, S. (2013). Cytochrome P450 CYP78A9 is involved in *Arabidopsis* reproductive development. Plant Physiol. **162**:779–799.

Trigueros, M., Navarrete-Gómez, M., Sato, S., Christensen, S.K., Pelaz, S., Weigel, D., Yanofsky, M.F., and Ferrándiz, C. (2009). The NGATHA genes direct style development in the *Arabidopsis* gynoecium. Plant Cell **21**:1394–1409.

Wu, H., Mori, A., Jiang, X., Wang, Y., and Yang, M. (2006). The INDEHISCENT protein regulates unequal cell divisions in *Arabidopsis* fruit. Planta **224**:971–979.

Yoshida, S., Barbier de Reuille, P., Lane, B., Bassel, G.W., Prusinkiewicz, P., Smith, R.S., and Weijers, D. (2014). Genetic control of plant development by overriding a geometric division rule. Dev. Cell **29**:75–87.